

Graph is a Natural Regularization: Revisiting Vector Quantization for Graph Representation Learning

Zian Zhai¹, Fan Li¹, Xingyu Tan¹, Xiaoyang Wang¹, Wenjie Zhang¹

¹University of New South Wales

zian.zhai@unsw.edu.au, fan.li8@unsw.edu.au, xingyu.tan@unsw.edu.au, xiaoyang.wang1@unsw.edu.au, wenjie.zhang@unsw.edu.au

Abstract

Vector Quantization (VQ) has recently emerged as a promising approach for learning discrete representations of graph-structured data. However, a fundamental challenge, i.e., codebook collapse, remains underexplored in the graph domain, significantly limiting the expressiveness and generalization of graph tokens. In this paper, we present the first empirical study showing that codebook collapse consistently occurs when applying VQ to graph data, even with mitigation strategies proposed in vision or language domains. To understand why graph VQ is particularly vulnerable to collapse, we provide a theoretical analysis and identify two key factors: early assignment imbalances caused by redundancy in graph features and structural patterns, and self-reinforcing optimization loops in deterministic VQ. To address these issues, we propose RGVQ, a novel framework that integrates graph topology and feature similarity as explicit regularization signals to enhance codebook utilization and promote token diversity. RGVQ introduces soft assignments via Gumbel-Softmax reparameterization, ensuring that all codewords receive gradient updates. In addition, RGVQ incorporates a structure-aware contrastive regularization to penalize the token co-assignments among similar node pairs. Extensive experiments demonstrate that RGVQ substantially improves codebook utilization and consistently boosts the performance of state-of-the-art graph VQ backbones across multiple downstream tasks, enabling more expressive and transferable graph token representations.

Introduction

In recent years, a discretization-based tokenization method, known as Vector Quantization (VQ), has attracted significant research attention for its effectiveness in generative modeling (Van Den Oord, Vinyals et al. 2017; Caron et al. 2018). VQ quantizes continuous latent representations into discrete clusters referred to as “codewords” in a learnable codebook. These codewords are then trained to reconstruct the original data samples. By discretizing the latent space, VQ provides an effective prior for learning disentangled features, and has achieved remarkable success in various generative modeling tasks, including image synthesis (Ramesh et al. 2021; Chang et al. 2023), speech generation (Dhariwal et al. 2020), and language models (Liu et al. 2025; Van Baalen et al. 2024).

Motivated by these successes, recent efforts have begun to explore the extension of VQ to graphs for scalable and versatile graph tokenization. First, discretizing graphs into VQ

tokens enables compact graph compression, substantially reducing the memory and computation overhead during inference (Yang et al. 2023; Luo et al. 2024). Second, VQ provides a natural mechanism for abstracting structural patterns into a reusable token vocabulary, analogous to the language tokens used in Large Language Models (LLMs), and offers a promising pathway toward Graph Foundation Models (GFMs) (Wang et al. 2024). Third, VQ allows graphs to be serialized into token sequences, enabling sequence-based modeling with standard Transformer architectures that are widely adopted in NLP and vision, and eliminating the need for handcrafted inductive biases that are typically required in Graph Transformers (Wang et al. 2025).

Observations. Similar to VQ models in the vision and language domains, which are typically trained to reconstruct input samples, Graph VQ is also trained with reconstruction objectives, i.e., node feature and link reconstruction. Nevertheless, through our empirical study, we observe that **codebook collapse** consistently occurs during the training, even when applying mitigation strategies that are commonly used in other domains. This refers to the phenomenon where most inputs are mapped to only a few codewords, leaving the majority underutilized (Zhu et al. 2024; Zhang et al. 2023). As a result, only a limited number of tokens can be utilized during inference, leading to overly coarse representations and significant degradation in performance. However, prior work focuses primarily on the performance of downstream tasks, without addressing this critical problem in the first place. This naturally leads to a central question: *What are the root causes that make Graph VQ more prone to collapse?*

Challenges. To answer this question, we investigate the phenomenon from both empirical and theoretical perspectives. Empirically, we find that the severity of collapse is correlated with typical graph properties such as structural and feature redundancy, indicating that inherent characteristics of graph data can aggravate the issue. Based on this observation, we theoretically identify two underlying factors: (1) early assignment imbalances caused by similar features and local structures; and (2) self-reinforcing training dynamics in VQ models, where frequently assigned codewords receive more updates and become increasingly dominant, while rarely selected ones remain inactive. This amplifies assignment imbalances and ultimately leads to collapse.

Solution. Based on these insights, we propose Regularized Graph VQ (RGVQ), a novel framework that integrates graph topology and feature similarity as explicit regularization signals to enhance codebook utilization. First, to break the self-reinforcing loops, RGVQ adopts the Gumbel-Softmax reparameterization to relax hard assignments into differentiable probability distributions, enabling the gradients to flow not only to the most likely codewords but also to the less probable candidates. Second, RGVQ leverages graph topology and feature similarity to regularize token assignment distributions, explicitly penalizing token co-assignments induced by graph redundancy. This regularization encourages nodes with similar features and local structures to share token distributions, while discouraging similar assignment among unrelated nodes. In summary, our main contributions can be briefed as follows.

- To the best of our knowledge, this is the first study to systematically investigate the problem of codebook collapse in graph data, a fundamental but underexplored challenge in discrete graph token learning.
- We conduct an empirical study on codebook collapse in Graph VQ and provide a theoretical analysis of its root causes from both data and optimization perspectives.
- We propose RGVQ, a novel framework that effectively addresses early token co-assignment bias by structure-aware regularization and disrupts the self-reinforcing dynamics in VQ training via stochastic quantization.
- We perform comprehensive experiments on state-of-the-art (SOTA) Graph VQ backbones, demonstrating that our proposed method improves codebook utilization and serves as a general solution for graph token learning.

Related Work

Vector Quantization. Vector Quantization (VQ) maps continuous inputs to discrete tokens in a codebook and has been widely used in image, video, and audio generation (Chung, Tang, and Glass 2020). This success has motivated efforts to extend VQ to graph data. For example, VQ-GNN (Ding et al. 2021) and VQGraph (Yang et al. 2023) apply VQ in supervised node classification tasks for embedding compression. However, their fully supervised training deviates from the original unsupervised training scheme of VQ. More recently, GFT pretrains VQ by reconstructing graph features to utilize the learned codebook as transferable vocabulary across tasks and domains (Wang et al. 2024). GQT employs residual VQ to tokenize graphs for vanilla transformers, alleviating manual architectural bias in graph transformers (Wang et al. 2025). While both methods demonstrate promising applications of Graph VQ, they overlook the issue of codebook collapse, which undermines the generalization of learned tokens. HQA-GAE introduces a hierarchical VQ with annealing for codeword selection, improving performance on graph tasks (Zeng et al. 2025). Nevertheless, it does not effectively resolve the non-differentiability of VQ and lacks a formal analysis of codebook collapse.

Collapse Mitigation. One of the most fundamental limitations of VQ is codebook collapse, wherein only a small

fraction of codewords are used. Various mitigation strategies have been explored in different domains. For example, Exponential Moving Average (EMA) is proposed to stabilize codebook updates. Pretraining the encoder (Zhao et al. 2024a) is proposed to mitigate embedding drift during training VQ. In addition, codebook reset (Zeghidour et al. 2021) periodically reinitializes inactive codewords with encoder embeddings. Affine parameters (Huh et al. 2023) introduce a learnable transformation before quantization to align encoder outputs with the codebook space and improve token utilization. Recently, SimVQ (Zhu et al. 2024) reparameterizes the code vectors through a linear transformation layer based on a learnable latent basis. Although these mitigation strategies have been evaluated in image and speech domains, their performance on graph data remains underexplored.

Preliminary

Graph Neural Network. Graph Neural Networks (GNNs) learn the node representations by recursively aggregating features from neighbors, also known as message-passing (Sun et al. 2022; Zhang et al. 2019). Formally, the representation of node v at the l -th layer is:

$$h_v^{(l)} = \text{AGG}(\{h_u^{(l-1)}, u \in \mathcal{N}(v) \cup v\}, \phi^{(l)}), \quad (1)$$

where $h_v^{(0)} = x_v$ is the initial node feature, $\mathcal{N}(v)$ is the neighbor set of node v , and $\phi^{(l)}$ is the parameters of the l -th layer of the GNN. The aggregation function $\text{AGG}(\cdot)$ combines the embedding of node v and its neighbors, which is typically implemented as sum, mean, or max pooling.

Deterministic VQ. VQ maps continuous representations into a finite set of discrete embeddings in the codebook (Van Den Oord, Vinyals et al. 2017). Given a codebook $\mathbf{C} = \{\mathbf{e}_i\}_{i=1}^K$ with each discrete codeword $\mathbf{e}_i \in \mathbb{R}^d$, a continuous input $h_i \in \mathbb{R}^d$ is quantized as z_i with the nearest codebook vector e_k by:

$$k = \arg \min_j \|h_i - \mathbf{e}_j\|_2^2 = \arg \min_j \|h_i - \delta_j \mathbf{C}\|_2^2, \quad (2)$$

where $\delta_j \in \{0, 1\}^{1 \times K}$ is the one-hot indicator vector with only the j -th element being 1. To enable gradient propagation through the non-differentiable vector δ_j , the Straight-Through Estimator (STE) is applied (Bengio, Léonard, and Courville 2013). During the backward process, the gradient of the quantized embedding $z_i = \delta_j \mathbf{C}$ is copied to h_i , which is denoted as

$$z_i = \text{sg}(\delta_j \mathbf{C} - h_i) + h_i, \quad \Rightarrow \quad \frac{\partial z_i}{\partial h_i} = 1, \quad (3)$$

where $\text{sg}[\cdot]$ denotes the stop-gradient operator. Finally, the learning objective is the combination of a reconstruction loss together with codebook loss and commitment loss that ensure the quantized codewords \mathbf{z} do not drift significantly from input embeddings \mathbf{h} :

$$\mathcal{L}_{\text{VQ}} = \underbrace{\mathcal{L}_{\text{recon}}}_{\text{reconstruction loss}} + \underbrace{\|\text{sg}[\mathbf{h}] - \mathbf{z}\|^2}_{\text{codebook loss}} + \beta \underbrace{\|\mathbf{h} - \text{sg}[\mathbf{z}]\|^2}_{\text{commitment loss}}. \quad (4)$$

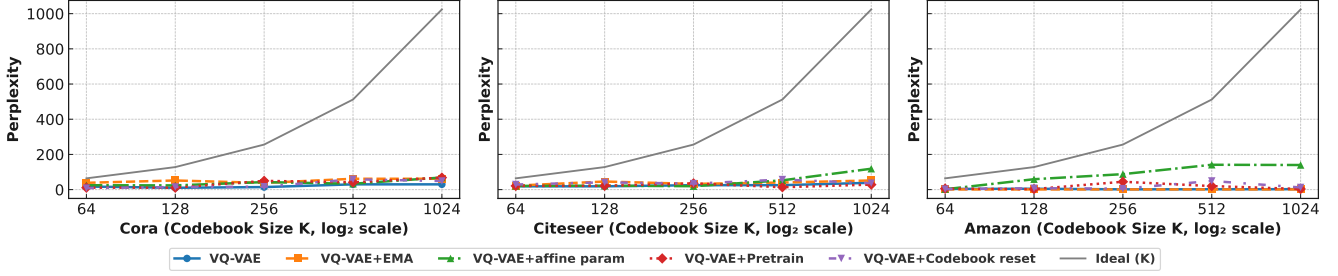


Figure 1: Codebook perplexities on graph datasets. The black lines indicate the optimal perplexities, i.e., codebook size K .

For Graph VQ, the reconstruction task typically involves reconstructing the graph properties, i.e., node features and links (Wang et al. 2024, 2025; Yang et al. 2023):

$$\mathcal{L}_{\text{recon}} = \underbrace{\frac{1}{N} \|D(\mathbf{z}) - \mathbf{X}\|_2^2}_{\text{feature reconstruction}} + \underbrace{\left\| \mathbf{A} - \sigma(\mathbf{z} \cdot \mathbf{z}^\top) \right\|_2^2}_{\text{link reconstruction}}, \quad (5)$$

where \mathbf{A} is the adjacency matrix, N is the total number of nodes, $D(\cdot)$ is the decoder, and \mathbf{X} is the node feature matrix. Note that there are other forms of loss functions, e.g., utilizing the negative sampling to compute the link reconstruction loss (Wang et al. 2024; Zeng et al. 2025).

Metric for Codebook Utilization. The extent of codebook collapse is measured by the codebook perplexity (Takida et al. 2022; Yan et al. 2024), which is defined as:

$$P = \exp \left(- \sum_{k=1}^K p_k \log p_k \right), \quad (6)$$

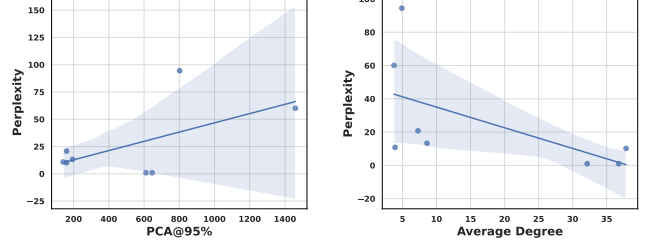
where p_k denotes the probability of selecting the k -th codeword. A low perplexity indicates that only a few codewords dominate the assignments, reflecting a high degree of collapse. In contrast, a high perplexity suggests better utilization of the codebook capacity.

Motivation

Recent studies demonstrate the potential of Graph VQ, while most focus on downstream performance, leaving codebook utilization largely underexplored. In this section, we conduct an empirical study of the codebook utilization and observe that codebook collapse occurs consistently during training, even when applying mitigation strategies from the language and vision domains. Moreover, we find that the severity of collapse correlates with the redundancy of graph data. Building on these observations, we provide a theoretical analysis and identify two key factors contributing to collapse: token co-assignments induces by similar features and local structures, and the self-reinforcing training dynamics of VQ models. These insights motivate the development of our method.

Empirical Study

We begin by investigating the codebook perplexity of Graph VQ on different graph datasets. Following the settings of



(a) PCA@95% vs. Perplexity (b) Avg. Degree vs. Perplexity

Figure 2: Correlation between graph properties and codebook perplexity.

prior work (Ding et al. 2021; Wang et al. 2024; Yang et al. 2023), we apply vanilla Graph VQ and its variants augmented with widely adopted collapse mitigation methods, including EMA, codebook reset, pretrained encoder, and affine parameters. By default, orthogonal normalization (Yu et al. 2021) and cosine similarities (Wang et al. 2024) are incorporated in all variants. More results and experiment settings can be found in Appendix A. From Figure 1, we make the following observations:

- Codebook collapse is a systematic and severe issue in Graph VQ. Across all datasets, the perplexity of VQ remains far below the codebook capacity, and fails to grow proportionally with the increasing codebook size.
- General mitigation strategies adopted from other domains only achieve marginal improvements and fail to fundamentally address codebook collapse in graphs.

These findings reveal that codebook collapse is not merely incidental, but a systematic issue in Graph VQ. We hypothesize that the unique properties of graph data, i.e., inherent feature redundancy and non-i.i.d. nature, may contribute to this phenomenon. To investigate this, we analyze two graph-level statistics that serve as proxies for these properties on different datasets. We consider: (1) PCA@95%, which quantifies feature redundancy by measuring the number of principal components needed to preserve 95% of node feature variance; and (2) average node degree, which reflects local connectivity density. Higher degrees imply stronger dependencies between neighboring nodes, violating the i.i.d. assumption and serving as a simple proxy for the non-i.i.d. nature of graph data (Yang et al. 2023). From Figure 2,

we observe a positive correlation between PCA@95% and codebook perplexity, and a negative correlation between average degree and perplexity. Lower PCA@95% suggests higher feature redundancy, and higher average degree implies stronger local connectivity and non-i.i.d. characteristics, both associated with a greater tendency toward collapse.

Theoretical Analysis

Assignment Imbalances. To better understand the mechanism behind the above observation, we provide a theoretical analysis that links graph redundancy to token assignment behavior. A key manifestation of codebook collapse is that nodes are increasingly mapped to the same codebook entry, regardless of their underlying differences. Thus, we begin by analyzing how the probability of two nodes being assigned to the same token is influenced by the similarity in terms of their features and local structures.

Theorem 1 (Token Co-assignment Probability with GNN Encoder). *Given two nodes v_1 and v_2 and their computation tree \mathcal{T}_{v_1} and \mathcal{T}_{v_2} , let $h_{v_1} = \phi(\mathcal{T}_{v_1})$, $h_{v_2} = \phi(\mathcal{T}_{v_2})$ be their embeddings under a GNN encoder ϕ with the distance between node embeddings $\Delta_{v_1, v_2}^L = \|h_{v_1} - h_{v_2}\|_2$. The probability that two nodes are quantized to the same codeword $p := \mathbb{P}[z_{v_1} = z_{v_2}]$ satisfies the following lower bound:*

$$p \geq \left(1 - \frac{1}{\delta_c} \left[C_1 \|x_{v_1} - x_{v_2}\|_2 + C_2 \sum_{j \in \mathcal{N}(v)} \Delta_{v_1, v_2, j}^{L-1} \right] \right) \geq \left(1 - \frac{2B_x}{\delta_c} \left[C_1 + \sum_{\ell=1}^L C_2^\ell D_\ell \right] \right), \quad (7)$$

where $\Delta_{v_1, v_2, j}^{L-1}$ denotes the distance between the $(L-1)$ -layer computation trees rooted at the j -th child of nodes v_1 and v_2 . $\delta_c > 0$ is the minimum distance from any codeword to the boundary of its Voronoi region. C_1, C_2 are constants, and B_x denotes bounded norm of node feature X . $D_\ell = d_\ell d_{\ell-1} \dots d_1$, and d_ℓ indicates the number of children of the ℓ -layer computation trees.

Proof. The proof can be found in Appendix B. \square

Remark 1. *Theorem 1 provides a theoretical interpretation of the empirical trends observed in Figure 2. When node features exhibit low variance or the graphs become more densely connected, the computation trees of different nodes become increasingly similar. This structural and feature redundancy increases the probability of token co-assignment, contributing to imbalanced codeword assignments.*

Self-Reinforcing Dynamics of Graph VQ. Given the higher probability of token co-assignments induced by graph data, we further analyze how the optimization dynamics of Graph VQ progressively amplifies imbalances and ultimately leads to collapse. In Graph VQ, the codebook \mathbf{C} is updated only through the vocabulary loss (Zhu et al. 2024), i.e., the second term in Equation 4. The update is denoted as:

$$\mathbf{C}^{(t+1)} = \mathbf{C}^{(t)} - \eta \mathbb{E}_{h_i} [\delta_k^\top \delta_k \mathbf{C}^{(t)}] + \eta \mathbb{E}_{h_i} [\delta_k^\top h_i], \quad (8)$$

where h_i is the embedding of node v_i , η is the learning rate, and $\delta_k^\top \delta_k$ is the Kronecker delta matrix, defined as:

$$(\delta_k^\top \delta_k)_{ij} = \begin{cases} 1 & \text{if } i = j = k, \\ 0 & \text{otherwise.} \end{cases} \quad (9)$$

This condition indicates that when the expectation $\mathbb{E}_{h_i} [\delta_k^\top \delta_k] = I$, i.e., every token is selected with equal probability $\frac{1}{K}$, each codebook entry is updated during training. However, according to Theorem 1, token assignments in graphs exhibit early imbalances. As a result, frequently selected codewords are more frequently updated and continuously pulled towards the distribution of the output of the GNN, i.e., \mathbf{h} . On the other hand, the encoder outputs are simultaneously optimized towards the selected codewords via the commitment loss in Equation 4. This hard assignment and bidirectional attraction form a self-reinforcing ‘‘co-con effect,’’ which not only locks the encoder into preferring codewords, but also suppresses any possibility of unused codewords being reactivated.

Methodology

Our analysis identifies that both the redundancy inherent in graph data and the self-reinforcing training dynamics of VQ as key factors contributing to codebook collapse. To address these challenges, we propose RGVQ, a regularized Graph VQ framework designed to mitigate collapse. The overall framework is illustrated in Figure 3. RGVQ first replaces hard assignments with differentiable assignment distributions using Gumbel-Softmax reparameterization, enabling gradients to flow to all codewords proportionally to their assignment probabilities. Building on this, RGVQ leverages graph topology and feature similarity to regularize token assignment distributions, explicitly penalizing co-assignment induced by graph redundancy.

Gumbel-Softmax Reparameterization. In deterministic VQ, the training dynamics of hard assignments prevent gradient backpropagation to unselected codewords, ultimately leaving them inactive and underutilized. To address this issue, we adopt Gumbel-softmax reparameterization (Roy et al. 2018; Sønderby, Poole, and Mnih 2017), which replaces hard nearest-neighbor assignment with a differentiable soft selection. Formally, the assignment distribution of quantizing h_i to entries in codebook \mathbf{C} is defined as:

$$p_i(\mathbf{C} | h_i) = \text{Softmax}(\pi), \quad \text{where } \pi = -\|h_i - \mathbf{C}\|^2. \quad (10)$$

Instead of using a non-differentiable argmax over the distribution, we apply the Gumbel-Softmax trick to estimate a differentiable approximation of this hard assignment. Specifically, the assignment distribution is perturbed with Gumbel noise and passed through a temperature-controlled softmax:

$$\tilde{p}_i(\mathbf{C} | h_i) = \text{Softmax}_\tau(\log p_i(\mathbf{C} | h_i) + g_i), \quad (11)$$

where $g_i \sim \text{Gumbel}(0, 1)$ is the sampled noise from Gumbel (0,1) and τ is the temperature. Given this estimated distribution, the quantized embedding is computed as a weighted average over all codebook entries:

$$\tilde{z}_i = \sum_{j=1}^K \tilde{p}_i(\mathbf{e}_j | h_i) \cdot \mathbf{e}_j, \quad \text{where } \mathbf{e}_j \in \mathbf{C}. \quad (12)$$

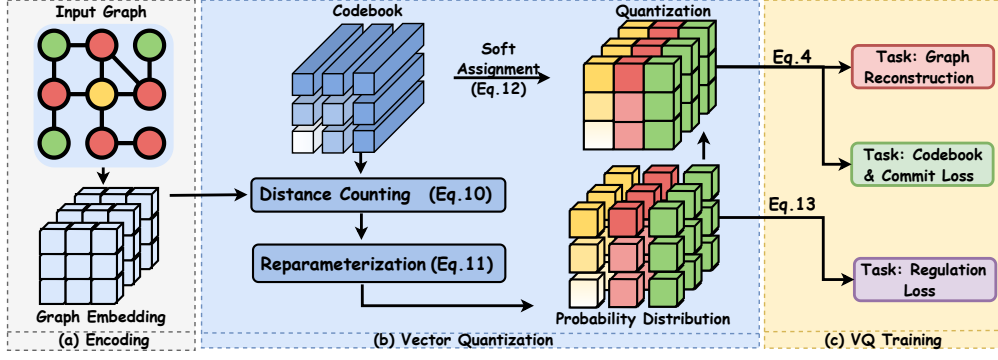


Figure 3: Overall framework of RGVQ. Note: red nodes represent the positive set, while green nodes denote negative samples.

This soft assignment allows all codebook entries to receive gradient updates proportionally to their participation in the quantized representation, thus mitigating the prementioned self-reinforced loop of deterministic VQ. During inference, the model reverts to deterministic hard assignment by selecting the codeword with the maximum logit $j = \arg \max_j p_i(\mathbf{C}|h_i)$.

Structure-Aware Regularization. To mitigate token co-assignments induced by the redundancy of graph data, we incorporate feature and structural similarities to regularize the token assignment distribution, encouraging the model to avoid overuse of specific codebook entries. Our key insight is that while structurally or semantically related nodes should share similar representations, they should nonetheless be assigned to distinct tokens to preserve codebook diversity. Thus, we distinguish between similar and dissimilar node pairs based on feature and structural similarity. Formally, for a given anchor node v , we define:

- **Positive set \mathcal{N}_P :** consists of the top-K nodes that are either structurally or semantically similar to v . Specifically, this includes nodes that satisfy at least one of the following conditions: (1) they are directly connected to v , i.e., $a_{uv} = 1$, where $a_{uv} \in A$ is the adjacency matrix; or (2) they have high feature similarity to v , i.e., $\|x_v - x_u\| < \epsilon$, where ϵ is a predefined threshold.
- **Negative set \mathcal{N}_N :** consists of the top-K nodes that are dissimilar to v in both structure and feature. Specifically, these are nodes that simultaneously satisfy: (1) they are not connected to v in the graph, i.e., $a_{uv} = 0$; and (2) they exhibit low feature similarity to v , i.e., $\|x_v - x_u\| > \gamma$, where $\gamma > \epsilon$.

We encourage nodes in the positive set to have similar assignment distributions, while penalizing nodes in the negative set for having overlapping token distributions. Formally, given two nodes v_i and v_j , we use \tilde{p}_i and \tilde{p}_j to represent their token assignment distributions $\tilde{p}_i(\mathbf{C} | h_i)$ and $\tilde{p}_j(\mathbf{C} | h_j)$ respectively. Then the distributions are regularized by an InfoNCE loss, which is defined as:

$$\mathcal{L}_i = -\log \frac{\sum_{j \in \mathcal{N}_P} \exp(\text{sim}(\tilde{p}_i, \tilde{p}_j))}{\sum_{j \in \{\mathcal{N}_P \cup \mathcal{N}_N\}} \exp(\text{sim}(\tilde{p}_i, \tilde{p}_j))}. \quad (13)$$

We average \mathcal{L}_i over all nodes to obtain the final regulation

loss, i.e., $\mathcal{L}_{\text{reg}} = \sum_N \mathcal{L}_i$. This regularization term is then added to the loss function in Equation 4, forming the ultimate loss for training Graph VQ:

$$\mathcal{L}_{\text{VQ}} = \mathcal{L}_{\text{recon}} + \|\text{sg}[\mathbf{h}] - \mathbf{z}\|^2 + \beta \|\mathbf{h} - \text{sg}[\mathbf{z}]\|^2 + \mathcal{L}_{\text{reg}}. \quad (14)$$

Connection to Other Works. Our proposed method leverages both feature and structural information as a regularization to promote codebook utilization in graph VQ models. It serves as a general solution for codebook collapse of Graph VQ, and can be utilized as a plugin for graph models that utilize VQ, e.g., GFT (Wang et al. 2024), GQT (Wang et al. 2025), and GraphVQ (Yang et al. 2023). Moreover, it is complementary with existing collapse mitigation strategies in other domains, e.g., EMA and codebook reset. Finally, this method can be seamlessly integrated into hierarchical VQ models such as Residual VQ (Luo et al. 2024), by incorporating the regularization at each layer.

Experiments

To evaluate the generality and effectiveness of RGVQ, in this section, we conduct extensive experiments based on three key functions of Graph VQ: (1) codebook utilization, (2) transferability, and (3) serialization. First, we evaluate the codebook utilization of RGVQ on both homophilous and heterophilous graphs, aiming to verify its ability to mitigate codebook collapse. Second, we investigate the transferability. We integrate RGVQ into GFT (Wang et al. 2024), a graph foundation model that utilizes the learned codebook as pretrained graph tokens, and evaluate the performance on cross-task and cross-domain graphs. Third, we assess the serialization capability of RGVQ by examining its compatibility with sequence-based models. We use GQT (Wang et al. 2025), a transformer that takes VQ tokens as input sequences, and evaluate the performance on node classification. Detailed dataset statistics, baselines, and implementation details are provided in Appendix C. The contrastive sets in RGVQ are pre-computed before training, we provide the complexity analysis in Appendix D.

Performance Evaluation

Codebook Utilization. We evaluate codebook utilization by comparing vanilla Graph VQ and its variants:

	Cora	PubMed	Citeseer	Photo	Computer	WikiCS	Ratings	Roman	Questions
Graph VQ	94.47	4.14	60.09	1.00	1.00	10.18	13.29	10.84	20.78
EMA	91.68	5.12	55.15	1.00	1.00	11.27	9.12	6.20	14.15
AP	75.32	126.55	9.03	54.95	59.33	83.55	73.82	118.46	66.57
Reset	65.79	102.78	85.19	10.73	17.18	134.44	130.83	150.51	141.98
PT	60.57	6.17	138.98	3.78	2.94	3.10	37.65	14.49	58.99
SimVQ	40.09	23.96	38.11	37.29	40.47	45.90	16.08	42.22	21.71
HQA-GAE	130.06	164.77	93.67	166.32	114.08	98.73	92.17	89.05	72.86
RGVQ	211.69	319.09	188.17	446.02	413.10	228.82	200.93	374.51	250.79

Table 1: Mean codebook utilization in perplexity on homophilous and heterophilous graphs with codebook size $K = 512$. **Bold** highlights the best performance. The model performance with standard deviation can be found in Appendix E.

Method	Node Classification			Link Classification		Graph Classification		
	Cora	PubMed	WikiCS	WN18RR	FB15K237	HIV	PCBA	Avg.
GCN	75.65	75.61	75.28	73.79	82.22	64.84	71.32	73.76
GAT	76.24	74.86	76.28	80.16	88.93	65.54	70.12	75.44
DGI	72.10	73.13	75.32	75.75	81.34	59.62	63.31	71.22
BGRL	71.20	75.29	76.53	75.44	80.66	63.95	67.09	72.67
GraphMAE	73.10	74.32	72.61	78.99	85.30	61.04	63.30	73.07
GFT	78.35	73.39	79.13	90.87	89.89	72.16	72.74	79.50
GFT + EMA	79.44	75.82	79.46	90.58	89.75	72.39	73.04	80.06
GFT + AP	79.69	74.03	78.05	89.56	89.05	71.86	71.48	79.10
GFT + Reset	80.07	73.56	79.73	91.18	88.09	72.79	71.95	79.62
GFT + PT	78.57	75.09	79.39	88.63	88.45	71.01	73.73	79.26
GFT + SimVQ	77.61	76.59	76.68	82.72	82.03	66.57	69.90	76.01
GFT + RGVQ	80.85	77.46	80.10	91.32	90.45	74.10	75.68	81.42

Table 2: Cross-domain and cross-task performance measured in Accuracy in the pre-training and fine-tuning setting. **Bold** highlight the best performance. Performance with standard deviation can be found in Appendix E.

EMA (Łańcucki et al. 2020), affine parameters (AP) (Huh et al. 2023), codebook reset (Reset) (Zeghidour et al. 2021), and pretrained encoders (PT) (Zhao et al. 2024a), as well as existing SOTA VQ models: SimVQ (Zhu et al. 2024) and HQA-GAE (Zeng et al. 2025). All methods use orthogonal normalization, cosine similarity, and K-Means initialization, and are trained on the feature and link reconstruction tasks. We fix the codebook size at 512 and report perplexity in Table 1. Across every dataset, RGVQ outperforms all baselines by a clear margin and remains robust, showing that Gumbel-Softmax reparameterization combined with structure-aware regularization leads to more balanced codebook use, prevents collapse, and enables more expressive graph representations. By contrast, vanilla Graph VQ and its variants suffer from severe codebook collapse, with perplexity values as low as 1.00 in several datasets. More advanced mitigation strategies like SimVQ and HQA-GAE offer only small improvements, indicating their limited ability to fundamentally address the underlying causes of collapse in Graph VQ.

Transferability. To evaluate the effectiveness of RGVQ in learning transferrable graph tokens, we integrate it into a graph foundation model, i.e., GFT, and compare it with vanilla Graph VQ and its variants with different mitiga-

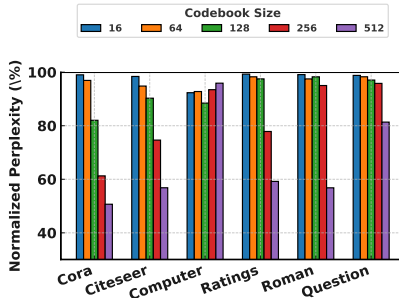
tion strategies. Moreover, we include supervised GNNs, i.e., GCN and GAT, and graph self-supervised methods, i.e., DGI (Veličković et al. 2018), BGRL (Thakoor et al. 2021), and GraphMAE (Hou et al. 2022). The supervised GNNs are trained directly on each target dataset, while the self-supervised methods and all GFT variants are pretrained on the full set of datasets and then fine-tuned per target.

Table 2 reports the model performance across cross-domain and cross-task datasets. RGVQ consistently achieves the highest average performance across all tasks and datasets, surpassing both supervised and self-supervised graph models, including GFT and its variants equipped with codebook collapse mitigation strategies. These consistent gains indicate that alleviating codebook collapse is essential for improving the expressiveness and transferability of graph tokens. By encouraging more balanced and diverse codebook utilization, RGVQ learns discrete representations that generalize better across tasks and domains, positioning it as a general and robust solution for GFMs.

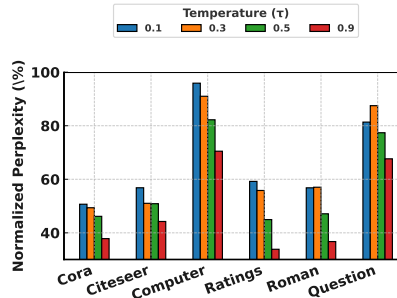
Serialization. To further evaluate the effectiveness of RGVQ in serialization, we integrate it into the Graph Quantized Transformer (GQT), where discrete tokens serve as the input sequence to a vanilla Transformer backbone. We

	Cora	PubMed	Citeseer	Photo	Computer	WikiCS	Ratings	Roman	Questions
GCN	75.65	75.61	73.14	96.10	93.99	75.28	53.80	91.27	79.02
GAT	76.24	74.86	72.22	96.60	94.09	76.28	55.54	90.63	77.95
GraphGPS	82.84	79.94	72.73	95.06	91.19	78.66	53.10	82.00	71.73
SGFormer	84.50	80.30	72.60	95.10	91.99	73.46	48.01	79.10	72.15
Expformer	82.77	79.46	71.63	95.35	91.47	78.54	53.51	89.03	-
GQT	86.44	81.60	73.14	94.46	92.13	80.03	54.04	89.85	76.52
GQT + RGVQ	88.34	86.54	81.25	97.66	95.67	83.58	55.16	90.98	78.26

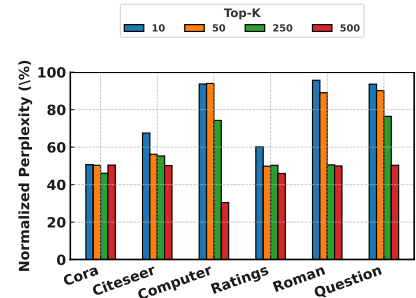
Table 3: Mean performance on node classification tasks. Metrics are reported in terms of ROC-AUC for Questions, and Accuracy for all other datasets. **Bold** indicates the best performance. Results with standard deviations are provided in Appendix E.



(a) Codebook size vs. Perplexity.



(b) Temperature (τ) vs. Perplexity.



(c) Top-K vs. Perplexity.

Figure 4: Ablation study results.

follow the original sequence reconstruction method (Wang et al. 2025) and compare the performance of RGVQ-enhanced GQT against the original GQT, supervised GNNs, and graph transformers, including GraphGPS (Rampášek et al. 2022), SGFormer (Wu et al. 2023), and Expformer (Shirzad et al. 2023). Table 3 summarizes the node classification results across various benchmarks. Compared to GQT, incorporating RGVQ consistently improves classification accuracy on most datasets. These results highlight the importance of mitigating codebook collapse when learning discrete tokens for Transformer-based architectures.

Ablation Studies

We further conduct ablation experiments on the contributions of the Gumbel–Softmax reparameterization and the structure-aware contrastive regularization.

Influence of the Codebook Size. We evaluate how codebook size affects the codebook utilization of RGVQ. The results are shown in Figure 4(a). Across all datasets, RGVQ consistently maintains high normalized perplexity as the codebook size increases, showing strong robustness to the choice of K . Notably, even with a large codebook size of 512, the model utilizes over 50% of the codebook capacity. This suggests that RGVQ can flexibly adapt to different representational granularities, and its token assignment remains stable even under large vocabulary settings.

Influence of the Temperature. We investigate how the Gumbel–Softmax temperature τ affects normalized perplex-

ity. As shown in Figure 4(b), lower temperatures, which produce distributions closer to one-hot, consistently improve codebook utilization. This indicates that, unlike some prior work (Zeng et al. 2025) that rely on temperature annealing, a relatively low and fixed temperature is sufficient to address the non-differentiability of deterministic VQ.

Influence of Contrastive Samples. We examine how the number of contrastive samples in structure-aware regularization affects normalized perplexity. As shown in Figure 4(c), even a small number of contrastive samples (e.g., $K = 10$ or 50) achieves relatively high normalized perplexity, indicating effective codebook use. Increasing K does not consistently lead to better utilization and may even degrade in some datasets, potentially due to added training noise.

Conclusion

In this paper, we investigate the codebook collapse problem in Graph VQ. Through empirical studies, we show that codebook collapse is not an incidental phenomenon, but a systematic issue of Graph VQ models. We provide a theoretical analysis of the underlying causes and propose RGVQ, a differentiable method that integrates both graph topology and feature similarity as explicit regulation signals to enhance codebook utilization and diversity. Extensive experiments demonstrate that RGVQ significantly mitigates codebook collapse and improves the downstream performance, highlighting its broad applicability in learning expressive and transferable graph representations.

References

- Bengio, Y.; Léonard, N.; and Courville, A. 2013. Estimating or propagating gradients through stochastic neurons for conditional computation. *arXiv preprint arXiv:1308.3432*.
- Caron, M.; Bojanowski, P.; Joulin, A.; and Douze, M. 2018. Deep clustering for unsupervised learning of visual features. In *Proceedings of the European conference on computer vision (ECCV)*, 132–149.
- Chang, H.; Zhang, H.; Barber, J.; Maschinot, A.; Lezama, J.; Jiang, L.; Yang, M.-H.; Murphy, K.; Freeman, W. T.; Rubinstein, M.; et al. 2023. Muse: Text-to-image generation via masked generative transformers. *arXiv preprint arXiv:2301.00704*.
- Chung, Y.-A.; Tang, H.; and Glass, J. 2020. Vector-quantized autoregressive predictive coding. *arXiv preprint arXiv:2005.08392*.
- Dhariwal, P.; Jun, H.; Payne, C.; Kim, J. W.; Radford, A.; and Sutskever, I. 2020. Jukebox: A generative model for music. *arXiv preprint arXiv:2005.00341*.
- Ding, M.; Kong, K.; Li, J.; Zhu, C.; Dickerson, J.; Huang, F.; and Goldstein, T. 2021. Vq-gnn: A universal framework to scale up graph neural networks using vector quantization. *Advances in Neural Information Processing Systems*, 34: 6733–6746.
- Hou, Z.; Liu, X.; Cen, Y.; Dong, Y.; Yang, H.; Wang, C.; and Tang, J. 2022. Graphmae: Self-supervised masked graph autoencoders. In *Proceedings of the 28th ACM SIGKDD conference on knowledge discovery and data mining*, 594–604.
- Huh, M.; Cheung, B.; Agrawal, P.; and Isola, P. 2023. Straightening out the straight-through estimator: Overcoming optimization challenges in vector quantized networks. In *International Conference on Machine Learning*, 14096–14113. PMLR.
- Łańcucki, A.; Chorowski, J.; Sanchez, G.; Marxer, R.; Chen, N.; Dolfing, H. J.; Khurana, S.; Alumäe, T.; and Laurent, A. 2020. Robust training of vector quantized bottleneck models. In *2020 International Joint Conference on Neural Networks (IJCNN)*, 1–7. IEEE.
- Liu, Z.; Luo, X.; Guo, J.; Ni, W.; Zhou, Y.; Guan, Y.; Guo, C.; Cui, W.; Feng, Y.; Guo, M.; et al. 2025. VQ-LLM: High-performance Code Generation for Vector Quantization Augmented LLM Inference. In *2025 IEEE International Symposium on High Performance Computer Architecture (HPCA)*, 1496–1509. IEEE.
- Luo, Y.; Li, H.; Liu, Q.; Shi, L.; and Wu, X.-M. 2024. Node Identifiers: Compact, Discrete Representations for Efficient Graph Learning. *arXiv preprint arXiv:2405.16435*.
- Ramesh, A.; Pavlov, M.; Goh, G.; Gray, S.; Voss, C.; Radford, A.; Chen, M.; and Sutskever, I. 2021. Zero-shot text-to-image generation. In *International conference on machine learning*, 8821–8831. Pmlr.
- Rampášek, L.; Galkin, M.; Dwivedi, V. P.; Luu, A. T.; Wolf, G.; and Beaini, D. 2022. Recipe for a general, powerful, scalable graph transformer. *Advances in Neural Information Processing Systems*, 35: 14501–14515.
- Roy, A.; Vaswani, A.; Neelakantan, A.; and Parmar, N. 2018. Theory and experiments on vector quantized autoencoders. *arXiv preprint arXiv:1805.11063*.
- Shirzad, H.; Velingker, A.; Venkatachalam, B.; Sutherland, D. J.; and Sinop, A. K. 2023. Expformer: Sparse transformers for graphs. In *International Conference on Machine Learning*, 31613–31632. PMLR.
- Sønderby, C. K.; Poole, B.; and Mnih, A. 2017. Continuous relaxation training of discrete latent variable image models. In *Bayesian Deep Learning workshop, NIPS*, volume 201.
- Sun, M.; Zhou, K.; He, X.; Wang, Y.; and Wang, X. 2022. Gpvt: Graph pre-training and prompt tuning to generalize graph neural networks. In *Proceedings of the 28th ACM SIGKDD Conference on Knowledge Discovery and Data Mining*, 1717–1727.
- Takida, Y.; Shibuya, T.; Liao, W.; Lai, C.-H.; Ohmura, J.; Uesaka, T.; Murata, N.; Takahashi, S.; Kumakura, T.; and Mitsufuji, Y. 2022. Sq-vae: Variational bayes on discrete representation with self-annealed stochastic quantization. *arXiv preprint arXiv:2205.07547*.
- Thakoor, S.; Tallec, C.; Azar, M. G.; Azabou, M.; Dyer, E. L.; Munos, R.; Veličković, P.; and Valko, M. 2021. Large-scale representation learning on graphs via bootstrapping. *arXiv preprint arXiv:2102.06514*.
- Van Baalen, M.; Kuzmin, A.; Koryakovskiy, I.; Nagel, M.; Couperus, P.; Bastoul, C.; Mahurin, E.; Blankevoort, T.; and Whatmough, P. 2024. Gptvq: The blessing of dimensionality for llm quantization. *arXiv preprint arXiv:2402.15319*.
- Van Den Oord, A.; Vinyals, O.; et al. 2017. Neural discrete representation learning. *Advances in neural information processing systems*, 30.
- Veličković, P.; Fedus, W.; Hamilton, W. L.; Liò, P.; Bengio, Y.; and Hjelm, R. D. 2018. Deep graph infomax. *arXiv preprint arXiv:1809.10341*.
- Wang, L.; Hassani, K.; Zhang, S.; Fu, D.; Yuan, B.; Cong, W.; Hua, Z.; Wu, H.; Yao, N.; and Long, B. 2025. Learning graph quantized tokenizers. In *The Thirteenth International Conference on Learning Representations*.
- Wang, Z.; Zhang, Z.; Chawla, N.; Zhang, C.; and Ye, Y. 2024. Gft: Graph foundation model with transferable tree vocabulary. *Advances in Neural Information Processing Systems*, 37: 107403–107443.
- Wu, Q.; Zhao, W.; Yang, C.; Zhang, H.; Nie, F.; Jiang, H.; Bian, Y.; and Yan, J. 2023. Sgformer: Simplifying and empowering transformers for large-graph representations. *Advances in Neural Information Processing Systems*, 36: 64753–64773.
- Yan, M.; Wu, J.; Shah, R.; and Liu, D. 2024. Gaussian Mixture Vector Quantization with Aggregated Categorical Posterior. *arXiv preprint arXiv:2410.10180*.
- Yang, L.; Tian, Y.; Xu, M.; Liu, Z.; Hong, S.; Qu, W.; Zhang, W.; Cui, B.; Zhang, M.; and Leskovec, J. 2023. Vqgraph: Graph vector-quantization for bridging gnns and mlps. *arXiv preprint arXiv:2308.02117*.

- Yu, J.; Li, X.; Koh, J. Y.; Zhang, H.; Pang, R.; Qin, J.; Ku, A.; Xu, Y.; Baldrige, J.; and Wu, Y. 2021. Vector-quantized image modeling with improved vqgan. *arXiv preprint arXiv:2110.04627*.
- Zeghidour, N.; Luebs, A.; Omran, A.; Skoglund, J.; and Tagliasacchi, M. 2021. Soundstream: An end-to-end neural audio codec. *IEEE/ACM Transactions on Audio, Speech, and Language Processing*, 30: 495–507.
- Zeng, L.; Yu, J.; Zhu, J.; Zhong, Q.; and Li, X. 2025. Hierarchical Vector Quantized Graph Autoencoder with Annealing-Based Code Selection. In *Proceedings of the ACM on Web Conference 2025*, 3772–3782.
- Zhang, J.; Zhan, F.; Theobalt, C.; and Lu, S. 2023. Regularized vector quantization for tokenized image synthesis. In *Proceedings of the IEEE/CVF Conference on Computer Vision and Pattern Recognition*, 18467–18476.
- Zhang, S.; Tong, H.; Xu, J.; and Maciejewski, R. 2019. Graph convolutional networks: a comprehensive review. *Computational Social Networks*, 6(1): 1–23.
- Zhao, W.; Zou, Q.; Shah, R.; and Liu, D. 2024a. Representation Collapsing Problems in Vector Quantization. *arXiv preprint arXiv:2411.16550*.
- Zhao, W.; Zou, Q.; Shah, R.; and Liu, D. 2024b. Representation Collapsing Problems in Vector Quantization. In *Neurips Safe Generative AI Workshop 2024*.
- Zhu, Y.; Li, B.; Xin, Y.; and Xu, L. 2024. Addressing representation collapse in vector quantized models with one linear layer. *arXiv preprint arXiv:2411.02038*.

Appendix

A. Empirical Study

Implementation Details. We provide the hyperparameters and experimental setup used in the empirical study of codebook perplexity. We jointly train the single-head VQ model and the GAT encoder using the link prediction and feature reconstruction tasks, along with the commitment loss and vocabulary loss. The task weights are set to 0.01, 100, 0.1, and 0.9, respectively. We train the model for 100 epochs and report the highest perplexity during the training process for each method and a specific codebook size K . For all methods, we utilize the kmeans initialization and orthogonal regularization for the codebook, with a regularization weight of 0.1. The GNN consists of 4 layers with a hidden dimension of 256. AdamW is utilized as the optimizer with a learning rate of $1e-4$ and a weight decay of $1e-5$. For affine parameters, we use Euclidean distance and set the codebook decay to 0.9. For codebook reset, the threshold of deadcode is set to 10. For pretraining encoder, we pretrain the GNN encoder for 50 epochs before the joint training.

Additional Experiments. In Figure 5, We provide the additional study of codebook perplexity across six datasets under varying codebook sizes, including both homophilous and heterophilous graphs. We report the study on Cora, Citeseer, and Amazon-computer in the main paper, and include PubMed, WikiCS, Amazon-Ratings, Roman-Empire, Questions, and Amazon-Photo in this appendix. Consistent with our main findings, all baseline methods exhibit severe collapse, failing to scale perplexity proportionally with the codebook capacity.

B. Proof of Co-assignment Bound

We restate Theorem 1 from the main paper as below.

Theorem 2 (Token Co-assignment Probability with GNN Encoder). *Given two nodes v_1 and v_2 and their computation tree \mathcal{T}_{v_1} and \mathcal{T}_{v_2} , let $h_{v_1} = \phi(\mathcal{T}_{v_1})$, $h_{v_2} = \phi(\mathcal{T}_{v_2})$ be their embeddings under a GNN encoder ϕ with the distance between node embeddings $\Delta_{v_1, v_2}^L = \|h_{v_1} - h_{v_2}\|_2$. The probability that two nodes are quantized to the same codeword $p := \mathbb{P}[z_{v_1} = z_{v_2}]$ satisfies the following lower bound:*

$$\begin{aligned} p &\geq \left(1 - \frac{1}{\delta_c} \left[C_1 \|x_{v_1} - x_{v_2}\|_2 + C_2 \sum_{j \in \mathcal{N}(v)} \Delta_{v_1, v_2, j}^{L-1} \right] \right) \\ &\geq \left(1 - \frac{2B_x}{\delta_c} \left[C_1 + \sum_{\ell=1}^L C_2^\ell D_\ell \right] \right), \end{aligned} \quad (15)$$

where $\Delta_{v_1, v_2, j}^{L-1}$ denotes the distance between the $(L-1)$ -layer computation trees rooted at the j -th child of nodes v_1 and v_2 . $\delta_c > 0$ is the minimum distance from any codeword to the boundary of its Voronoi region. C_1, C_2 are constants, and B_x denotes bounded norm of node feature X . $D_\ell = d_\ell d_{\ell-1} \dots d_1$, and d_ℓ indicates the number of children of the ℓ -layer computation trees.

Proof. Since the GNN encoder is based on message passing, each node’s embedding depends on information aggregated from its local neighborhood. This process can be formalized as a computation tree \mathcal{T}_v^L of depth L , rooted at node v , where messages are propagated from leaf nodes up to the root. The embedding h_v can thus be viewed as a function of this tree, i.e., $h_v = \phi(\mathcal{T}_v^L)$. Let x_v denote the node feature of v and \mathcal{N}_v be the set of its direct neighboring nodes, which correspond to the children of the computation tree \mathcal{T}_v^L . We begin by computing the embedding distance between two L -layer computation trees (Wang et al. 2024), whose embeddings are generated by the GNN ϕ with parameters $\mathbf{W} = (\mathbf{W}_1, \mathbf{W}_2)$, where \mathbf{W}_1 and \mathbf{W}_2 are the transformation of the root node and its neighboring nodes, respectively. Note that both \mathbf{W}_1 and \mathbf{W}_2 are Lipschitz continuous and are bounded by $\|\mathbf{W}_1\| < \mathcal{B}_{\mathbf{W}_1}$ and $\|\mathbf{W}_2\| < \mathcal{B}_{\mathbf{W}_2}$. For simplicity, we assume that the GNN parameters are shared across all layers, i.e., \mathbf{W} remains the same at each layer, which does not affect the validity of the proof. Then the node embedding is computed as: $h_v =$

$$\phi(\mathcal{T}_v^L) = \sigma \left(\mathbf{W}_1 x_v + \mathbf{W}_2 \rho \left(\sum_{j \in \mathcal{N}(v)} g(\mathcal{T}_j^{L-1}(\mathbf{W})) \right) \right), \quad (16)$$

where σ is the activation function, ρ is the permutation-invariant aggregation, and g is the update function in neural networks. For simplicity, we use $\mathcal{T}_v^L(\mathbf{W})$ to represent $\phi(\mathcal{T}_v^L)$.

Then, we have the lower bound of the distance between node embeddings $\Delta_{v_1, v_2}^L =:$

$$\begin{aligned} \|\mathcal{T}_{v_1}^L(\mathbf{W}) - \mathcal{T}_{v_2}^L(\mathbf{W})\|_2 &= \|\sigma(\mathbf{W}_1 x_{v_1} + \mathbf{W}_2 R(\mathcal{T}_{v_1})) \\ &\quad - \sigma(\mathbf{W}_1 x_{v_2} + \mathbf{W}_2 R(\mathcal{T}_{v_2}))\|_2 \\ &\leq C_\sigma \|\mathbf{W}_1(x_{v_1} - x_{v_2}) \\ &\quad + \mathbf{W}_2(R(\mathcal{T}_{v_1}) - R(\mathcal{T}_{v_2}))\|_2 \\ &\leq C_\sigma \|\mathbf{W}_1(x_{v_1} - x_{v_2})\|_2 \\ &\quad + C_\sigma \|\mathbf{W}_2(R(\mathcal{T}_{v_1}) - R(\mathcal{T}_{v_2}))\|_2 \\ &\leq C_\sigma \mathcal{B}_{\mathbf{W}_1} \|x_{v_1} - x_{v_2}\|_2 \\ &\quad + C_\sigma \mathcal{B}_{\mathbf{W}_2} \|R(\mathcal{T}_{v_1}) - R(\mathcal{T}_{v_2})\|_2 \end{aligned} \quad (17)$$

where $R(\mathcal{T}_v) := \rho \left(\sum_{j \in \mathcal{N}(v)} g(\mathcal{T}_j^{L-1}(\mathbf{W})) \right)$. Considering the Lipschitz continuity of ρ and g , then $\|R(\mathcal{T}_{v_1}) - R(\mathcal{T}_{v_2})\|_2$ is bounded as:

$$\begin{aligned} \|R(\mathcal{T}_{v_1}) - R(\mathcal{T}_{v_2})\|_2 &\leq C_\rho \left\| \sum_{j \in \mathcal{N}(v)} g(\mathcal{T}_{v_1, j}^{L-1}) - g(\mathcal{T}_{v_2, j}^{L-1}) \right\|_2 \\ &\leq C_\rho \sum_{j \in \mathcal{N}(v)} \|g(\mathcal{T}_{v_1, j}^{L-1}) - g(\mathcal{T}_{v_2, j}^{L-1})\|_2 \\ &\leq C_\rho C_g \sum_{j \in \mathcal{N}(v)} \|\mathcal{T}_{v_1, j}^{L-1} - \mathcal{T}_{v_2, j}^{L-1}\|_2 \\ &= C_\rho C_g \sum_{j \in \mathcal{N}(v)} \Delta_{v_1, v_2, j}^{L-1}, \end{aligned} \quad (18)$$

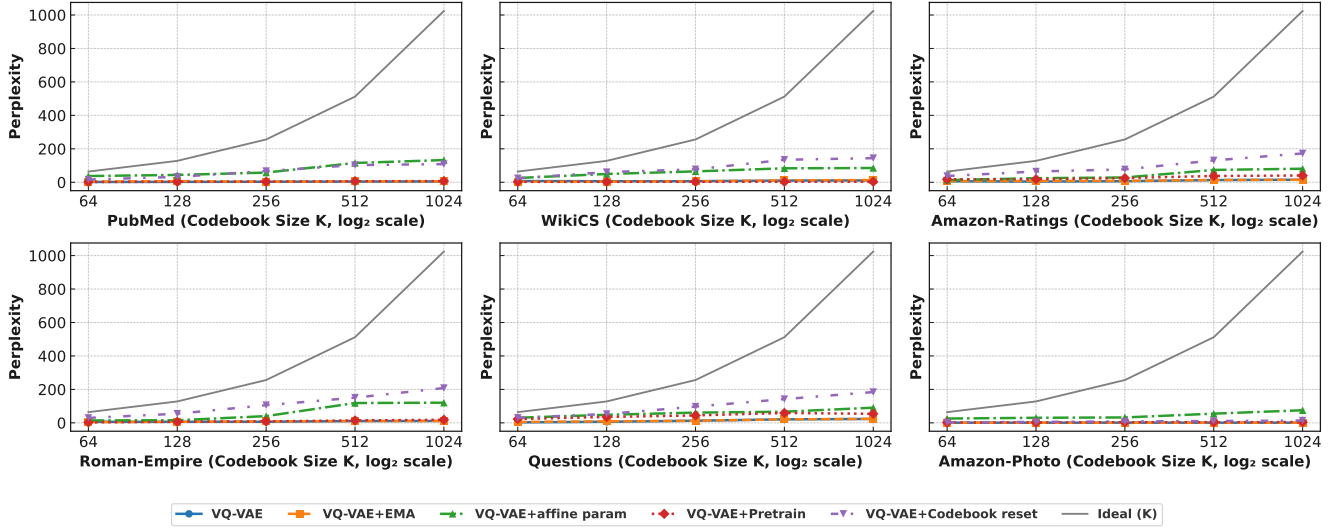


Figure 5: Codebook perplexities on graph datasets. The black lines indicate the optimal perplexities, i.e., codebook size K .

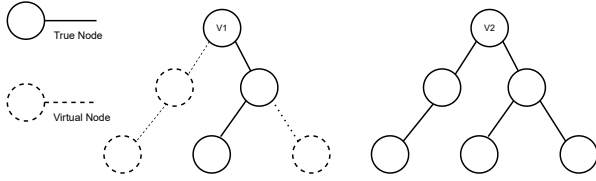


Figure 6: Adding virtual nodes to align the computation trees of v_1 and v_2 .

where $\Delta_{v_1, v_2, j}^{L-1} = \|\mathcal{T}_{v_1}^{L-1}(\mathbf{W}) - \mathcal{T}_{v_2}^{L-1}(\mathbf{W})\|_2$ is the distance of the embeddings between the j -th child of nodes v_1 and v_2 . Here we assume that v_1 and v_2 have the same local structures by padding virtual nodes in their actual computation trees, as shown in Figure 6, such that the j -th child of both v_1 and v_2 always exists. These virtual nodes do not have features and do not affect the actual computation and the generality of the proof. Let d_l denote the number of branches, i.e., number of children at the l -th layer, the bound in Equation 4 can be simplified as:

$$\|R(\mathcal{T}_{v_1}) - R(\mathcal{T}_{v_2})\|_2 \leq C_\rho C_g d_{l-1} \max_{j \in \mathcal{N}(v)} \Delta_{v_1, v_2, j}^{L-1}. \quad (19)$$

This bound indicates that the most influential child of a node, i.e., a largely connected node will dominate all other children, and allows us to repeatedly expand $\Delta_{v_1, v_2, j}^{L-1}$ until the leaf nodes, where the distance is directly computed between input node features. Specifically, by recursively applying the above bound over tree depth L , we have:

$$\Delta_{v_1, v_2}^L \leq C_1 \|x_{v_1} - x_{v_2}\|_2 + C_2 d_{l-1} \max_{j \in \mathcal{N}(v)} \Delta_{v_1, v_2, j}^{L-1}, \quad (20)$$

where $C_1 = C_\sigma \mathbf{B}_{\mathbf{W}_1}$ and $C_2 = C_\sigma \mathbf{B}_{\mathbf{W}_2} C_\rho C_g$ are constants. Given all node features X are bounded by $\|X\|_2 \leq \mathcal{B}_x$ and the distance of x_{v_1} and x_{v_2} are bounded by $\|x_{v_1} - x_{v_2}\| \leq$

$2\mathcal{B}_x$. We further develop the bound as:

$$\Delta_{v_1, v_2}^L \leq 2\mathcal{B}_x \left(C_1 + \sum_{\ell=1}^L C_2^\ell D_\ell \right), \quad (21)$$

where $D_\ell = d_\ell d_{\ell-1} \cdots d_1$ denotes the total branching factor up to depth ℓ .

Then, we develop the lower bound of token co-assignment based on the computation tree of v_1 and v_2 . Let z_{v_1} and z_{v_2} be the quantized tokens assigned via codebook \mathcal{C} . For the lower bound, we consider the sufficient condition for token co-assignment. Let r_c denote the minimum distance between any two distinct codewords in the codebook. We define the codeword safety radius as $\delta_c = \frac{r_c}{2} > 0$. This radius r_c guarantees that any pair of embeddings within distance δ_c must lie entirely within the Voronoi region of the same codeword, and hence be quantized to the same token. Therefore, the following implication holds:

$$\Delta_{v_1, v_2}^L \leq \delta_c \Rightarrow z_{v_1} = z_{v_2}. \quad (22)$$

Therefore, a sufficient condition for co-assignment is that their embedding distance is less than or equal to δ_c . Then:

$$\mathbb{P}[z_{v_1} = z_{v_2}] \geq \mathbb{P}[\|h_{v_1} - h_{v_2}\| \leq \delta_c]. \quad (23)$$

Using Markov's inequality on the non-negative random variable $\|h_{v_1} - h_{v_2}\|$ gives:

$$\mathbb{P}[\|h_{v_1} - h_{v_2}\| > \delta_c] \leq \frac{\mathbb{E}[\|h_{v_1} - h_{v_2}\|]}{\delta_c}. \quad (24)$$

Then, we derive lower bound of the probability that two nodes are assigned to the same token as:

$$\mathbb{P}[\|h_{v_1} - h_{v_2}\| \leq \delta_c] \geq 1 - \frac{\|h_{v_1} - h_{v_2}\|}{\delta_c} = 1 - \frac{\Delta_{v_1, v_2}^L}{\delta_c}. \quad (25)$$

We use p to simply represent $\mathbb{P}[\|h_{v_1} - h_{v_2}\|]$. According to Equation 20 and 21, we substitute Δ_{v_1, v_2}^L with their upper bound and have:

$$\begin{aligned} p &\geq \left(1 - \frac{1}{\delta_c} \left[C_1 \|x_{v_1} - x_{v_2}\|_2 + C_2 \sum_{j \in \mathcal{N}(v)} \Delta_{v_1, v_2, j}^{L-1} \right] \right) \\ &\geq \left(1 - \frac{2B_x}{\delta_c} \left[C_1 + \sum_{\ell=1}^L C_2^\ell D_\ell \right] \right), \end{aligned} \quad (26)$$

Note that this lower bound is a conservative estimate of the true co-assignment probability. This is because the bound only accounts for embedding pairs whose distance is within δ_c , which is a sufficient condition for co-assignment. The actual probability may be higher. There may exist additional cases where $\|h_{v_1} - h_{v_2}\| > \delta_c$ but both embeddings still fall within the Voronoi region of the same codeword, such that $z_{v_1} = z_{v_2}$ still holds. \square

C. Experiments

Datasets. We use both homophilous and heterophilous graphs in our experiments. To evaluate codebook utilization, we use various datasets, including Cora, CiteSeer, PubMed, Amazon-Computer, Amazon-Photo, WikiCS, Amazon-Ratings, and Roman-Empire. To assess transferability, we use cross-task and cross-domain datasets. Specifically, we use Cora, PubMed, and WikiCS for node classification; WN18RR and FB15K237 for link prediction; and HIV and PCBA for graph classification. Finally, we evaluate serialization ability using the same datasets employed for codebook utilization. Detailed dataset statistics are summarized in Table 4.

Baselines. We use different baselines for three parts of our main experiments.

- **Codebook Utilization.** We primarily adopt codebook mitigation strategies originally developed in the vision and language domains, including EMA (Łańcucki et al. 2020), affine parameters (Huh et al. 2023), codebook reset (Zeghidour et al. 2021), and pretrained encoders (Zhao et al. 2024b). We further include SimVQ (Zhu et al. 2024), which addresses the codebook collapse via one-single MLP layer over the latent basis vectors. Additionally, we compare with HQA-GAE (Zeng et al. 2025), a recent graph VQ model that applies a hierarchical VQ structure and an annealing strategy for codeword selection.
- **Transferability.** To evaluate the effectiveness of RGVQ in learning transferrable graph tokens, we integrate it into a graph foundation model, i.e., GFT, and compare it with vanilla Graph VQ and its variants with different mitigation strategies. Moreover, we include supervised GNNs, i.e., GCN and GAT, and graph self-supervised methods, i.e., DGI (Veličković et al. 2018), BGRL (Thakoor et al. 2021), and GraphMAE (Hou et al. 2022). The supervised GNNs are trained directly on each target dataset, while

the self-supervised methods and all GFT variants are pre-trained on the full set of datasets and then fine-tuned per target.

- **Serialization.** To further evaluate the effectiveness of RGVQ in serialization, we integrate it into the Graph Quantized Transformer (GQT) (Wang et al. 2025), where discrete tokens serve as the input sequence to a vanilla Transformer backbone. We follow the original sequence reconstruction method and compare the performance of RGVQ-enhanced GQT against the original GQT, supervised GNNs, and graph transformers, including GraphGPS (Rampášek et al. 2022), SGFormer (Wu et al. 2023), and Exphomer (Shirzad et al. 2023).

Implementation Details. We provide the hyperparameters and implementation details of our main experiments.

- **Codebook Utilization.** The implementation of all collapse mitigation strategies is the same with the empirical study (see Appendix A). For HQA-GAE, we use one-head VQ model and use the same hidden dimension and number of GNN layers as other methods, while all remaining hyperparameters follow the original paper. For RGVQ, we set the codebook size K to 512, and sample 20 contrastive examples for both the positive and negative sets. The training weights for the link prediction, node feature reconstruction, contrastive regularization, commitment loss, and vocabulary loss are set to 0.01, 100, 1, 0.1, and 0.9, respectively. We set the temperature for the Gumbel-Softmax trick to 0.1.
- **Transferability.** We use RGVQ as a plugin within the pretraining pipeline of GFT. Specifically, we retain the link, node feature, and tree embedding reconstruction tasks and integrate RGVQ with respective weights of 100, 1, 0.01, and 10. For all other configurations, including downstream fine-tuning in GFT, we strictly follow the settings from the original paper (Wang et al. 2024).
- **Serialization.** We pretrain RGVQ using the same configuration as in the codebook utilization experiments for 200 epochs. We then load the pretrained checkpoints, including the codebook, GNN encoder, and VQ module weights. We follow the hyperparameter settings from the original GQT paper (Wang et al. 2025).

D. Complexity Analysis

Assume a L -layer GNN, a codebook of size K , and hidden dimension of d , the number of nodes and links are denoted as $|\mathcal{V}|$ and $|\mathcal{E}|$ respectively. We divide the complexity analysis into two parts: Pre-computation of contrastive set and quantization process.

Pre-computation of Contrastive Set. Before training, RGVQ constructs for each node sets of positive and negative samples, based on both structural and feature similarity. This step is performed once and reused during training. To implement this, neighbors are first extracted by scanning the adjacency matrix, which requires $O(|\mathcal{E}|)$ time. Then compute feature distances between each node and all others will take $O(|\mathcal{V}|^2 d)$ time. However, in practice, we adopt

Dataset	Domain	Task	# Graphs	Avg. #Nodes	Avg. #Edges	# Classes
CiteSeer	Citation	Node	1	3,327	4,522	6
Cora	Citation	Node	1	2,708	10,556	7
PubMed	Citation	Node	1	19,717	88,651	3
Computer	Co-purchase	Node	1	13,752	491,722	10
Photo	Co-purchase	Node	1	7,650	238,163	8
WikiCS	Web link	Node	1	11,701	216,123	10
Amazon-Ratings	Review	Node	1	22,662	32,927	18
Roman-Empire	Synthetic	Node	1	24,492	93,050	5
Questions	Synthetic	Node	1	48,921	153,540	2
FB15K237	Knowledge	Link	1	14,541	310,116	237
WN18RR	Knowledge	Link	1	40,943	93,003	11
PCBA	Molecule	Graph	437,929	26.0	28.1	128
HIV	Molecule	Graph	41,127	25.5	27.5	2

Table 4: Dataset statistics for selected datasets.

	Cora	PubMed	Citeseer	Photo	Computer	WikiCS	Ratings	Roman	Questions
Graph VQ	94.47 ±8.65	4.14 ±1.03	60.09 ±5.59	1.00 ±0.00	1.00 ±0.00	10.18 ±2.13	13.29 ±2.89	10.84 ±3.48	20.78 ±3.65
EMA	91.68 ±9.17	5.12 ±1.46	55.15 ±6.73	1.00 ±0.00	1.00 ±0.00	11.27 ±3.36	9.12 ±2.33	6.20 ±3.24	14.15 ±3.51
AP	75.32 ±6.28	126.55 ±12.64	9.03 ±2.16	54.95 ±5.43	59.33 ±8.55	83.55 ±9.86	73.82 ±8.14	118.46 ±16.21	66.57 ±8.27
Reset	65.79 ±8.56	102.78 ±15.78	85.19 ±4.41	10.73 ±1.98	17.18 ±2.37	134.44 ±7.35	130.83 ±8.88	150.51 ±11.15	141.98 ±10.11
PT	60.57 ±10.25	6.17 ±1.12	138.98 ±10.54	3.78 ±1.37	2.94 ±1.27	3.10 ±1.31	37.65 ±5.76	14.49 ±2.52	58.99 ±8.34
SimVQ	40.09 ±6.53	23.96 ±2.56	38.11 ±6.67	37.29 ±4.85	40.47 ±6.54	45.90 ±7.35	16.08 ±4.11	42.22 ±8.34	21.71 ±5.27
HQA-GAE	130.06 ±5.52	164.77 ±14.15	93.67 ±11.32	166.32 ±10.98	114.08 ±10.15	98.73 ±7.82	92.17 ±8.66	89.05 ±8.23	72.86 ±7.79
RGVQ	211.69 ±5.27	319.09 ±10.40	188.17 ±11.23	446.02 ±15.82	413.10 ±10.78	228.82 ±5.96	200.93 ±7.89	374.51 ±11.13	250.79 ±8.63

Table 5: Mean codebook utilization in perplexity on homophilous and heterophilous graphs with codebook size $K = 512$. **Bold** highlights the best performance.

a sampling strategy: for each node, we sample M non-neighbor nodes (where M is a small constant, e.g., 100) and compute their feature similarity. This limits the total cost of semantic similarity computation to $O(|\mathcal{V}| \cdot M \cdot d)$, which is linear in the number of nodes. After collecting both structurally and semantically similar candidates, we perform top- k selection for each node to finalize its positive sample set, costing $O(|\mathcal{V}| \log k)$ time in total. Negative samples are the same from all nodes. Thus, the overall time complexity of the contrastive set construction process is $O(|\mathcal{E}| + |\mathcal{V}| \cdot M \cdot d + |\mathcal{V}| \log k)$, which is linear in the number of nodes and edges under fixed M and k .

Quantization Process. The time and space complexity of the GNN encoder are $O(Ld^2|\mathcal{V}| + Ld|\mathcal{E}|)$ and $O(Ld^2 + Ld|\mathcal{V}| + |\mathcal{E}|)$, respectively. The decoder has the same complexity. RGVQ computes the distance between each node embedding and all K codewords, and estimates the soft as-

signment distribution via the Gumbel-Softmax trick. This process requires $O(|\mathcal{V}|Kd)$ time and $O(|\mathcal{V}|K)$ space. Finally, RGVQ regularizes the assignment distributions using the InfoNCE loss between node pairs. For each node, this involves computing similarities with k positive and k negative samples, each over K -dimensional distributions. The total cost is $O(|\mathcal{V}| \cdot (2k) \cdot K)$.

E. Results with Deviations

We run each methods 5 times and provide the mean performance with standard deviations for codebook utilization, transferability, and serialization ability in Table 5, Table 6, and Table 7 respectively.

Method	Node Classification			Link Classification		Graph Classification		Avg.
	Cora	PubMed	WikiCS	WN18RR	FB15K237	HIV	PCBA	
GCN	75.65 ± 1.37	75.61 ± 2.10	75.28 ± 1.34	73.79 ± 0.39	82.22 ± 0.28	64.84 ± 4.78	71.32 ± 0.49	73.76
GAT	76.24 ± 1.62	74.86 ± 1.87	76.28 ± 0.78	80.16 ± 0.27	88.93 ± 0.15	65.54 ± 6.93	70.12 ± 0.89	75.44
DGI	72.10 ± 0.34	73.13 ± 0.64	75.32 ± 0.95	75.75 ± 0.59	81.34 ± 0.15	59.62 ± 1.21	63.31 ± 0.89	71.22
BGRL	71.20 ± 0.30	75.29 ± 1.33	76.53 ± 0.69	75.44 ± 0.30	80.66 ± 0.29	63.95 ± 1.06	67.09 ± 1.00	72.67
GraphMAE	73.10 ± 0.40	74.32 ± 0.33	72.61 ± 0.39	78.99 ± 0.48	85.30 ± 0.16	61.04 ± 0.55	63.30 ± 0.78	73.07
GFT	78.35 ± 1.07	73.39 ± 1.68	79.13 ± 0.32	90.87 ± 0.25	89.89 ± 0.27	72.16 ± 1.69	72.74 ± 1.23	79.50
GFT + EMA	79.44 ± 0.89	75.82 ± 1.32	79.46 ± 0.58	90.58 ± 0.43	89.75 ± 0.19	72.39 ± 1.52	73.04 ± 1.01	80.06
GFT + AP	79.69 ± 1.07	74.03 ± 0.92	78.05 ± 0.58	89.56 ± 0.18	89.05 ± 0.18	71.86 ± 1.53	71.48 ± 0.99	79.10
GFT + Reset	80.07 ± 0.91	73.56 ± 0.85	79.73 ± 0.63	91.18 ± 0.43	88.09 ± 0.23	72.79 ± 1.65	71.95 ± 0.85	79.62
GFT + PT	78.57 ± 0.86	75.09 ± 1.21	79.39 ± 0.89	88.63 ± 0.15	88.45 ± 0.17	71.01 ± 1.74	73.73 ± 1.12	79.26
GFT + SimVQ	77.61 ± 0.73	76.59 ± 1.07	76.68 ± 0.76	82.72 ± 0.53	82.03 ± 0.35	66.57 ± 1.35	69.90 ± 0.91	76.01
GFT + RGVQ	80.85 ± 0.73	77.46 ± 0.94	80.10 ± 0.52	91.32 ± 0.26	90.45 ± 0.31	74.10 ± 1.49	75.68 ± 0.99	81.42

Table 6: Cross-domain and cross-task performance measured in Accuracy in the pre-training and fine-tuning setting. **Bold** highlights the best performance.

	Cora	PubMed	Citeseer	Photo	Computer	WikiCS	Ratings	Roman	Questions
GCN	75.65 ± 1.37	75.61 ± 2.10	73.14 ± 0.67	96.10 ± 0.46	93.99 ± 0.12	75.28 ± 1.34	53.80 ± 0.60	91.27 ± 0.20	79.02 ± 0.60
GAT	76.24 ± 1.62	74.86 ± 1.87	72.22 ± 0.84	96.60 ± 0.33	94.09 ± 0.37	76.28 ± 0.78	55.54 ± 0.51	90.63 ± 0.14	77.95 ± 0.51
GraphGPS	82.84 ± 1.03	79.94 ± 0.26	72.73 ± 1.23	95.06 ± 0.13	91.19 ± 0.54	78.66 ± 0.49	53.10 ± 0.42	82.00 ± 0.61	71.73 ± 1.47
SGFormer	84.50 ± 0.80	80.30 ± 0.60	72.60 ± 0.20	95.10 ± 0.47	91.99 ± 0.76	73.46 ± 0.56	48.01 ± 0.49	79.10 ± 0.32	72.15 ± 1.31
Expformer	82.77 ± 1.38	79.46 ± 0.35	71.63 ± 1.19	95.35 ± 0.22	91.47 ± 0.17	78.54 ± 0.49	53.51 ± 0.46	89.03 ± 0.37	-
GQT	86.44 ± 1.58	81.60 ± 1.35	73.14 ± 1.26	94.46 ± 0.68	92.13 ± 0.23	80.03 ± 0.19	54.04 ± 0.12	89.85 ± 0.73	76.52 ± 1.52
GQT + RGVQ	88.34 ± 1.32	86.54 ± 1.41	81.25 ± 1.01	97.66 ± 1.05	95.67 ± 0.36	83.58 ± 0.66	55.16 ± 0.29	90.98 ± 0.66	78.26 ± 1.07

Table 7: Mean performance on node classification tasks. Metrics are reported in terms of ROC-AUC for Questions, and Accuracy for all other datasets. **Bold** indicates the best performance.